Sustained antibody response to ZIKV infection induced by NS1 protein is accompanied by the progressive appearance of autoreactive antibodies and cross-reactive B cell clones.

Cecilia B. Cavazzoni[1,2], Vicente B. T. Bozza[1], Lucas Tostes[1], Bruno Maia[3], Luka Mesin[2], Ariën Schiepers[2], Jonatan Ersching[2,†], Romulo L.S. Neris[3], Jonas N. Conde[4], Diego R. Coelho[4], Luciana Conde[1], Heitor de Paula Neto[5], Tulio M. Lima[6], Renata G.F. Alvim[6], Leda R. Castilho[6], Ronaldo Mohana-Borges[4], Iranaia Assunção-Miranda[3], Alberto Nobrega[3], Gabriel D. Victora[2], Andre M. Vale[1,*]

[1] Laboratório de Biologia de Linfócitos, Instituto de Biofísica Carlos Chagas Filho, Universidade Federal do Rio de Janeiro, Rio de Janeiro, RJ, 21941-590, Brazil

[2] Laboratory of Lymphocyte Dynamics, The Rockefeller University, New York, NY, USA

[3] Instituto de Microbiologia Paulo de Góes, Universidade Federal do Rio de Janeiro, Rio de Janeiro, Brazil

[4] Laboratório de Genômica Estrutural, Instituto de Biofísica Carlos Chagas Filho, Universidade Federal do Rio de Janeiro, Rio de Janeiro, RJ, 21941-590, Brazil

[5] Laboratório de Alvos Moleculares, Faculdade de Farmácia, Universidade Federal do Rio de Janeiro, Rio de Janeiro, Brazil

[6] Programa de Engenharia Química, Laboratório de Engenharia de Cultivos Celulares (LECC), COPPE, Universidade Federal do Rio de Janeiro, Rio de Janeiro (UFRJ), Cx. Postal 68502, Rio de Janeiro,RJ 21941-972, Brazil

[†] *In memoriam*

*Correspondence to André M. Vale: valeam@biof.ufrj.br

Abstract

Antibodies are key players in controlling viral infections. However, in addition to antigen-specific responses to viral antigens, humoral immune response can generate polyreactive and autoreactive antibodies of unknown function. Dengue and Zika virus infections have been linked to autoimmune disorders including Guillain-Barrè syndrome. A unique feature of flaviviruses is the secretion of non-structural protein 1 (NS1) by infected cells. NS1 is highly immunogenic and antibodies targeting NS1 can have both protective and pathogenic roles. In the present study, we investigated the humoral immune response to Zika virus NS1 and found NS1 to be an immunodominant viral antigen correlated to the presence of autoreactive antibodies. Through single B cell cultures, we coupled binding assays and BCR sequencing, confirming the immunodominance of NS1 and the presence of self-reactive clones in germinal centers both after infection and immunization, some of which were cross-reactivity with NS1. Anti-NS1 B cell clones showed features related to pathogenic autoreactive antibodies. Our findings demonstrate NS1 immunodominance at the cellular level as well as a potential role for NS1 in ZIKV associated autoimmune manifestations.

Introduction

The protective function of antibodies is instrumental for the control of most viral infections. However, in addition to antigen-specific responses to viral antigens, it has long been noted that viral infection can be accompanied by the appearance of polyreactive and often autoreactive antibodies of unknown function [1]. Emergence of self-reactive immunoglobulins has been reported for multiple viral diseases. These have the potential to lead to autoimmune manifestations, which can be transient or long-lasting (reviewed in [2]). The origin of the stimulus driving autoantibody generation in viral infection remains controversial; antigen mimicry between viral and self-antigens may well explain the appearance of some autoantibodies, although a role for non-specific, polyclonal B cell activation has also been considered [3]. Other work suggests that non-specific, polyclonal B cell activation with hyperglobulinemia could result in disruption of B cell repertoire homeostasis, thus breaking self-tolerance [1].

Recently, dengue virus (DENV) and zika virus (ZIKV) infections have been linked to the occurrence of autoimmune disorders of vascular, ophthalmic or neurological origin, including Guillain-Barrè syndrome [4, 5], in which autoantibodies seem to play a prominent role [6]. A unique feature of DENV, ZIKV and other flaviviruses is the abundant secretion of the hexameric non-structural protein 1 (NS1) by infected cells [7-10]. While intracellular NS1 was shown to be necessary for the transcription and replication of the virus, its role as an extracellular soluble factor is poorly understood [11]. Work from multiple groups has shown that NS1 is highly immunogenic [12-14]. Of note, antibodies to DENV NS1 can attenuate the presentation of severe dengue. Similarly, vaccination with ZIKV and DENV NS1 have been shown to be protective in animal models [15-17]. These studies suggest a role for NS1 in the pathogenesis of flavivirus infections, as well as a protective role for anti-NS1 antibodies. However, anti-DENV NS1 antibodies have also been implicated in autoreactivity and may contribute to dengue pathology, suggesting the possibility of antigen mimicry between NS1 and components of self [18-22]; these observations raise concerns about the safety of NS1 as a vaccine antigen, and further studies are necessary to understand the humoral immune response to this molecule.

Studies of the pathogenesis of human viral infections in animal models can be challenging, and for this reason, multiple groups have developed models that rely on immunocompromised mice, such as IFNAR-deficient strains, which show greater susceptibility to viral infection [23-26]. Although such strategies are useful in studies of viral pathology, they are less useful for the analysis of humoral immune responses, as type-I interferons broadly influence acquired immunity and directly impact the activation of B cells by modulating B cell receptor (BCR) signaling [27, 28] . Using mouse models, we and others have shown that CD4+ T cells activate

a robust IFNγ-dependent B cell response, which is associated with production of neutralizing IgG2a antibodies that bind to ZIKV envelope proteins including envelope protein domain III (EDIII) and have been associated with virus neutralization. Passive transfer of serum from infected A129 mice, which retain IFNγ signlaning, protected immunocompromised mice against lethal challenge with a different strain of ZIKV [29-31]. In addition to interferons, other cytokines and signals such as toll-like receptor (TLR) ligands present during infection influence B cell activation and selection within germinal centers (GCs), and a role for type I interferons cannot be excluded. For these reasons, an immunocompetent mouse model of ZIKV infection is preferred for the study of antibody response. Accordingly, recent studies have used such models to characterize the T cell [32-34] and neutralizing antibody response to ZIKV [35].

In the present study, we investigated the humoral immune response to NS1 using an immunocompetent mouse model of ZIKV infection as well as NS1 immunization. We found NS1 to be an immunodominant viral antigen and correlated the antibody response to this protein with the presence of autoreactive antibodies after infection. In-depth analysis coupling single B cell cultures with BCR sequencing confirmed the strong immunodominance of NS1 and revealed the presence of frequent self-reactive clones among GC B cells, some of which were cross-reactivity with NS1. Anti-NS1 B cell clones were enriched in charged amino acid residues in the CDR-H3 region, a feature also shared by self-reactive clones. Anti-NS1 clones also showed low levels of somatic hypermutation (SHM) suggesting a possible adaptation of the germline repertoire towards this antigen. Importantly, our data show engagement of self-reactive B cells in GCs formed in response to an immunodominant viral antigen, suggesting a break of tolerance at the cellular level. These findings highlight the potential relevance of NS1 for ZIKV pathogenicity and its associated autoimmune manifestations as well as the importance of evaluating the B cell repertoire in its entirety.

Results

Immunocompetent BALB/c mice develop a specific antibody response to ZIKV infection focused on NS1.

To study the humoral immune response to ZIKV infection in immunocompetent mice, we injected young adult BALB/c WT mice intravenously with 10^7-10^8 PFU of the Brazilian ZIKV isolate PE243 [36] and followed antibody responses for 50 days post-infection (d.p.i) (Fig. 1 A). Mice showed increased spleen weight on days 7 to 28 after infection (Fig. 1 B), as well as altered total serum immunoglobulin concentrations. Increased serum IgM was detected at 7 d.p.i. (Fig. 1 C) and total serum IgG concentration increased progressively between 7 and 21 d.p.i., after which it stabilized at a higher concentration than controls for up to 50 days after infection (Fig. 1 D).

Serum IgM binding to envelope proteins peaked at 7 d.p.i. (Fig. 1 E) followed by a peak of IgG at 14 d.p.i., (Fig. 1 F) as detected using Zika virus-like particles (VLPs) that display proteins E and M in their mature form [37]. Domain III of protein E (EDIII) is a target of neutralizing antibodies for different flaviviruses [35, 38-40] and we therefore also looked for serum IgG binding to this portion of protein E. We found that EDIII specific IgG peaked in serum at 14 d.p.i. (Fig. 1 G) at which point serum neutralization capacity was also observed (Fig. 1 H).

We next searched for NS1-binding IgM and IgG antibodies in the sera of infected mice. NS1 is known to be abundantly secreted into the extracellular milieu by flavivirus-infected cells [41] and is highly immunogenic [8]. IgM binding to NS1 remained almost unchanged compared to noninfected mice (Fig. 1 I). Interestingly, although the appearance of serum IgG targeting NS1 occurs later than that binding to envelope proteins, anti-NS1 IgG increased progressively after infection, remaining at very high levels as long as 50 d.p.i. (Fig. 1 J) and 60 d.p.i. (Fig. S1 C). Taken together, these results demonstrate that, although immunocompetent mice survive ZIKV infection with few or no clinical signs, infection was able to induce a robust humoral immune response, which became progressively dominated by antibodies to the NS1 antigen.

Dominance of NS1-binding IgG in serum correlates with the emergence of autoreactive antibodies

The increasing levels of anti-NS1 IgG antibodies from 21 d.p.i. onwards prompted us to further investigate the NS1-specific response in infected mice. Serum titration, at different time points, suggested an increase in concentration or affinity of IgG for the viral antigen (Fig. 2 A). Endpoint titers increased gradually to approximately 200,000 at the latest evaluated time point (Fig. 2 B). Serum IgG was predominantly of the IgG2a isotype throughout infection, as expected for anti-viral responses [42]. Of note, the contribution of IgG1 to total serum IgG titer was delayed compared to other isotypes (Fig. 2 C and D). Given that gamma 1 constant region gene is located upstream of gamma 2a, ruling out sequential switching between these isotypes, our data suggest continued engagement of B cell clones after the initial phase of the response.

We then assessed the binding of IgG to closely-related dengue virus antigens. As observed in human antibody response to ZIKV infection [14, 43], we found cross-reactivity between ZIKV EDIII and DENV EDIII (Fig. 2 E; Fig. S1, A and B), whereas ZIKV NS1 specific IgG did not cross-react with DENV NS1 protein (Fig. 2 F; Fig. S1, C and D). In addition to the presence of virus-specific antibody responses, viral infections are often associated with hyperglobulinemia due to non-specific polyclonal activation of B lymphocytes [1]. To assess the potential of ZIKV infection to induce a polyclonal, non-specific humoral response, we

looked for IgG binding to unrelated antigens such as heat shock proteins from both mammals and commensal bacterial origins, which are commonly targeted by autoantibodies in different systems [44-46] (Fig. S1, E and F). IgG binding to unrelated antigens, possibly due to polyreactivity, was present at early time points and rapidly decayed, following the kinetics of antibody response to viral structural proteins as detected using VLPs (see Fig. 1, F and G). Interestingly, serum Ig from ZIKV-infected mice also displayed widespread binding to self-antigens, as revealed using a semiquantitative immunoblot assay that enables global analysis of the self-reactivity of antibodies present in serum [47, 48]. Accordingly, at 14 d.p.i., ZIKV-infected mice exhibited serum IgG reactivity to multiple self-antigens from syngeneic brain and muscle tissues (Fig. 2 G, left lanes), suggesting a break in self-tolerance during the early humoral immune response. Representative data of global analysis of autoreactive antibodies from two individual mice following ZIKV infection are shown in Figure 2, G-J.

Polyclonal B cell activation and non-specific polyreactive responses are mainly present in the acute phase of the immune response to viral infections, and do not contribute meaningfully to serum IgG titers at later time points, after viremia subsides. These considerations prompted us to evaluate whether self-antigen reactivity declines at later time points after infection. Strikingly, serum IgG self-reactivity was progressively stronger at later time points (Fig. 2, G-I). Of note, although different mice shared several reactivities towards antigens with similar migration patterns in the blot (Fig. 2, G and H), individual immunoreactivity profiles did not necessarily converge in time towards a unique reactivity profile (Fig. 2 J).

To further confirm the progressive increase of self-reactive IgG following infection, we tested serum samples from an additional cohort of ZIKV-infected mice for binding to a HEp-2 cell line extract. These cells are frequently used in standard clinical assays for anti-nuclear antibodies (ANAs), but also as a source for cytoplasmic self-antigens [49]. Consistently, a broad range of immunoreactivities arose over time after infection (Fig. 2 K). The increase in IgG reactivity to a 60 kDa self-antigen paralleled reactivity towards NS1 (Fig. 2 L). The coincidence of the kinetics of anti-NS1 response and the progressive reinforcement of serum IgG self-reactivity led us to hypothesize a possible link between the maintenance of autoreactive antibodies and a dominant and sustained anti-NS1 antibody response.

The GC response contains both virus-specific and autoreactive clones.

Viral infections typically induce T-dependent antibody responses, in which follicular B cells (FO) enter GC reactions where they undergo B cell clonal expansion, SHM, and antibody affinity maturation (reviewed in [50]). We found significant alterations in the frequencies of splenic FO and GC B cells over time. The reduction in frequency of FO B cells reflected GC formation and correlated with levels of serum IgG specific to ZIKV proteins. GC B cell

frequency peaked at day 14 after infection and started to decrease at day 21, receding to background levels at 28 d.p.i. (Fig. 3 A).

To investigate a possible link between the antibody response to NS1 and the presence of self-reactive IgG, we devised an experimental strategy that allowed us to easily compare GC B cells between different infected and immunized mice. Mice were subcutaneously infected in the footpad with ZIKV, and draining lymph nodes (LN) were collected on different days post-infection to isolate GC B cells (Fig. 3 B). Consistent with our previous results, we found increasing levels of IgG binding to ZIKV NS1 in serum up to 45 days after footpad infection. This increase was not observed when the same amount of UV-inactivated virus (iZIKV) was injected into the footpad, indicating that our model involves productive ZIKV infection (Fig. 3 C). We could also observe GC formation in LN after both ZIKV infection and iZIKV injection, although the latter were of lesser magnitude both in frequency of GC B cells and in duration of the GC response (Fig. 3, D and E). At 14 d.p.i., corresponding to the peak of the response, we isolated and cultured GC B cells for Ig production *in vitro*. GC B cell cultures were performed as described by Kuraoka et al.[51], with modifications, including not adding IL-4 to prevent *in vitro* class switching. As a result, the proportions of IgG isotypes found in culture supernatants broadly matched those of the ZIKV-specific antibodies in serum (data not shown).

Through limiting dilution assay (LDA), we were able to estimate the frequency of GC B cells secreting immunoglobulins binding to VLP or NS1 (Fig. 3, F and G), as well as to self-antigens (Fig. 3 H). The precise quantification of the number of responding B cell clones per culture ensures accurate determination of the frequency of GC B cells reactive to a given antigen [52, 53]. GC B cells from mock-, iZIKV-, and ZIKV-injected mice showed similar frequencies of response to polyclonal stimuli, with 30% to 50% of GC B cells proliferating and differentiating into IgG-secreting plasma cells in all conditions. At 14 d.p.i., less than 0.1% of GC B cells from iZIKV-injected mice secreted IgG that bound detectably to VLP. Moreover, we were unable to detect GC B cell clones secreting NS1-reactive IgG in neither mock- nor iZIKV-injected mice (data not shown). On the other hand, in ZIKV-infected mice, GC B cells specific for NS1 were readily detected at relatively high frequencies (Fig. 3 F). The proportion of GC B cells reacting with NS1 (4.5%) was 10-fold higher than that of GC B cells binding to envelope proteins (0.4%) (Fig. 3 G), commensurate with virus-specific IgG levels observed in serum (Fig. 3 C; see also Fig. 1, F and J). These findings underscore the extent of the immunodominance of NS1 over envelope antigens also at the cellular level.

We then performed the same global analysis of self-reactivities used for serum IgG (Fig. 2 H) with GC B cell culture supernatants. By combining LDA and immunoblot assays, we were able to estimate the frequency of IgG binding to selected antigens in each GC B cell

culture (Fig. 3 H). Our analysis showed that autoreactive B cells were present within GCs formed after exposure to replicative ZIKV, but were virtually absent upon exposure to UV-inactivated virus (Fig. 3 H). Importantly, the self-reactivity found with highest frequency (Ag2) accounted for 1% of GC B cells in the lymph node (Fig. 3 H), at least twice the frequency of GC B cells detectably specific for virus envelope proteins (Fig. 3 G). These data suggest a role for NS1 in triggering the autoreactive antibody response following ZIKV infection.

ZIKV NS1 immunization recruits a high frequency of NS1-specific B cells to the GC

To directly implicate the anti-NS1 humoral immune response in the generation of autoreactive antibodies, we immunized mice in the footpad with purified recombinant ZIKV NS1 in the presence of a TLR7 agonist (R848). Control groups included mice immunized with ZIKV envelope proteins (E and M) in the form of VLPs in the presence of R848. An additional group of mice was immunized with a combination of VLPs and NS1 (Fig. 4 A). We first analyzed the humoral immune response against the viral antigens. We found that, from day 14 post-immunization onwards, serum levels of NS1-specific IgG were higher than those of VLP-specific IgG in both combinations (Fig. 4 B). Despite the similar frequencies of total GC B cells in popliteal LNs (Fig. 4 C), frequencies of specific B cells within the GC varied. At day 14 after immunization with VLP/R848, the frequency of GC B cells binding to VLP was 2.6% (Fig. 5 E, left panels). After immunization with NS1 and adjuvant, however, the frequency of specific GC B cells was approximately 10-fold higher, at 27% (Fig. 4 E, right panels). Compared to the single antigen immunization protocol, VLP and NS1 in combination reduced the frequency of GC B cells specific for both antigens to 1.2% and 3%, respectively. (Fig. 4E, middle panels). On the other hand, similar levels of NS1 specific IgG were found in culture supernatants, irrespective whether VLPs were present in the immunization or not (Fig. 4F). Altogether, specific GC B cell frequency and kinetics in immunized mice mirrored the virus-specific IgG levels found in the ZIKV infection model, further supporting the observed immunodominance of NS1 over ZIKV envelope antigens.

Paucity of SHM but increased frequency of charged CDR-H3s in B cell clones from ZIKV NS1-immunized mice

To further characterize the B cell response to ZIKV NS1, we sorted and sequenced single GC B cells from popliteal LNs of mice immunized with this antigen at different time points. To gain insight into specific features of ZIKV NS1, we also immunized mice with DENV NS1 for comparison, since the two proteins are structurally homologous but nevertheless antibodies generated after infection with ZIKV do not cross-react with DENV NS1 (see Fig. 2 F). As expected GCs found in popliteal LNs of mice immunized with either ZIKV or DENV NS1 proteins at 10 days post-immunization were highly clonally diverse, whereas clones with increased frequency accumulated over time (Fig. 5A).

Analysis of VH gene usage showed preferential use of the VH1 (J558) gene family, irrespective of immunizing antigen and time point analyzed (data not shown). The average number of mutations in VH gene segments was similar for both antigens and increased over time as one would expect. However, interestingly, VH mutation numbers were lower among larger clones (likely those undergoing positive selection) in GCs formed after ZIKV NS1 immunization when compared to those formed after DENV NS1 immunization (Fig. 5 B). In contrast to those from ZIKV NS1 immunization, B cells in GCs from DENV NS1-immunized mice tended to progressively accumulate mutations in the more expanded clones over time (Fig. 5 B). The lower number of somatic mutations in B cell clones from ZIKV NS1 immunization suggested that the germline repertoire of BABL/c mice may already be enriched for clones with sufficient binding affinity towards ZIKV NS1.

Although no significant differences in CDR-H3 length were found in GC B cells after DENV or ZIKV NS1 immunization at any time point (Fig. 5 C), there was a preference for 11-amino acid-long CDR-H3s in both ZIKV NS1 and DENV NS1 immunized mice when compared to the naïve B cell repertoire (Fig. 5 D). Average CDR-H3 hydrophobicity tended to be lower for ZIKV NS1 than for DENV NS1 (Fig. 5 E). The distribution of CDR-H3 average hydrophobicities revealed few highly charged sequences among B cells responding to ZIKV NS1 antigen (Fig. 5 F). Comparison of the amino acid composition of this region for both antigens at each time point revealed an enrichment over time for charged amino acids, especially arginine after ZIKV NS1 immunization (Fig. 5 G). Of note, charged amino acids in the antigen binding sites of IgG are often critical for self-reactivity [54]. However, a marked glycine (neutral amino acid) enrichment was also observed, which could counterbalance the charged amino acid bias, resulting in a moderate change in average hydrophobicity in CDR-H3 sequences as shown in Fig. 5 E. Evaluating the difference between hydrophobic and charged amino acids by CDR-H3 sequence, we found that the ZIVK NS1 immunized B cell repertoire indeed used charged amino acids more frequently than hydrophobic ones in individual CDR-H3 sequences when compared to the DENV NS1 immunized B cell repertoire (Fig. 5 H).

The recruitment of B cells enriched in charged CDR-H3 sequences into the GCs upon immunization with ZIKV NS1 may be related to the emergence of autoreactive IgG. However, it is worth noting that the specificities of the immunoglobulins encoded by these sequences are not known. The results obtained with cultures of GC B cells suggest that most of these cells (63% for ZIKV NS1 and 97% for ZIKV VLP) do not secrete antibodies with detectable affinity to the antigen used in immunization (Fig. 4 E). One might expect that the most expanded clones would be those with the greatest affinity for the antigen; however, it remains possible that the most mutated clones would become expanded only at later time points, after more extensive selection, and would therefore fail to be detected at high frequencies in the

samples analyzed. To better understand this phenomenon, we sought to correlate the features of immunoglobulin variable gene sequences with the specificities of their secreted antibodies.

ZIKV NS1 immunization induces GC B cell clones enriched for charged CDR-H3s and self-reactivity

To understand the relationship between Ig sequence features and binding properties, we used single GC B cell cultures, which allow the assessment of both *Ig* sequence and binding properties from the same cell (adapted from [53]). We first determined the frequency of GC B cell clones secreting ZIKV NS1-binding IgG from popliteal LNs of mice at different time points after immunization. In line with the rising levels of serum IgG specific to NS1 (shown in Fig. 4 B), frequency of ZIKV NS1-specific B cells also increased over time, from an average of 30% at 10 days to 50% at 21 days post-immunization (Fig. 6 A). We then divided B cell clones into NS1-binders and non-binders for further analyses. Clonal expansion was evident among NS1-binder B cells, peaking on day 14 after immunization (when almost 60% of NS1-binder B cells belonged to expanded clonotypes), consistent with antigen-driven selection (Fig. 6 B). At day 21 p.i., the fraction of expanded clones among NS1-binders decayed to levels similar to those found at day 10 post-immunization, suggesting continued ingress of new B cell clones into ongoing GCs (Fig. 6 B). In contrast, non-binder clones were stable and showed significantly less clonal expansion at all time points analyzed (Fig. 6 B). Interestingly, and consistent with the data shown previously (Fig. 5 B), we did not find evidence for positive selection of NS1-binding clones bearing large numbers of somatic hypermutations (Fig. 6 C).

We then sought to investigate the physicochemical features of the CDR-H3 sequences expressed by the B cell clones recruited to GCs by ZIKV NS1 immunization. On day 14 p.i., both ZIKV NS1 binders and non-binders showed similar CDR-H3 hydrophobicity, whereas on day 21 p.i., ZIKV NS1 binders tended to be less charged and closer to neutrality than non-binders, an effect just short of statistical significance (Fig. 6 D). To examine whether NS1 binding correlated with the abundance of positively charged amino acids in CDR-H3, we plotted the anti-NS1 reactivity per clone at each time point, highlighting CDR-H3s expressing three or more charged amino acids (Fig. 6 E). CDR-H3 sequences bearing charged amino acids were frequent and evenly distributed among NS1-binder and non-binder clones, accounting for 25% to 35% of the CDR-H3 sequences (Fig. 6 E).

A common feature associated with self-reactivity is the presence of positively charged amino acids within CDR-H3 [55]. To determine whether specific *Ig* sequence features were correlated with self-reactivity, we tested 60 antibodies for binding to autologous muscle and brain extracts (Table S1). Corroborating the results obtained with serum and limiting dilution of GC B cells, no self-reactivity was found among GC B cells from mice immunized with DENV

NS1 at any time point (Table S1). In contrast, 12% of single cells obtained at day 14 after immunization with ZIKV were self-reactive, including one clone found twice with different SHM patterns. This frequency increased to 38% at 21 d.p.i., when several clones were found as variants with different SHM patterns, such as the clone bearing the glycine enriched CDR-H3 ARGGGFDGFAY, which lost self-reactivity by acquiring a non-silent mutation that led to the replacement of a phenylalanine by a tyrosine (becoming ARGGGYDGFAY). Another interesting autoreactive clone carried the ARGTLYAMDY CDR-H3 which, in addition to being among the most hydrophobic sequences in our list, was also found in both a more mutated but non-autoreactive (ARGTLYTMDY) and a more mutated autoreactive (ARGTLYSMDY) form (Table S1). Both clones in all their variants also bound to ZIKV NS1 protein.

Clones found at the highest frequencies bound ZIKV NS1 and were generally not self-reactivity, although some NS1 binders that cross-reacted with self-antigens were expanded to a lesser extent, suggesting that antigen-specific GC B cells – whether self-reactive or not – could undergo positive selection. Interestingly, all NS1-binding immunoglobulins tested for self-reactivity, regardless of their self-reactivity, had numbers of VH mutations that were similar and higher than those of non-antigen-specific cells, again suggesting antigen-driven selection (Fig. 6 F). The least mutated clones were those that were self-reactive but did not bind to ZIKV NS1 protein (Fig. 6 G). Accordingly, these clones were exclusively found as singletons (Fig. 6 G).

The results obtained with single cell sequencing and binding assays are summarized in Figure 6H. In the first column, clonality scores show that the presence of more expanded clones is a property of earlier GCs, obtained at day 14 post-infection, whereas late GCs were enriched in smaller clones. Interestingly, the decrease in clonal dominance inversely correlated with increased self-reactivity, suggesting a replacement of early clones by a new wave of B cells with self-reactive potential. Collectively, SHM appears not to increase from day 14 to 21p.i., which would be in line with clonal replacement. Self-reactive clones are apparent already on day 14p.i., all of which exhibit cross-reactivity with ZIKV NS1. It is interesting to note that autoreactive clones with no cross reactivity with NS1 are present at day 21p.i. but not at day 14 p.i. A distinctive feature of CDR-H3 sequences of GC B cells from ZIKV infected or ZIKV NS1 immunized mice is the strong enrichment for presence of charged amino acids, which is well above the value observed for the naïve repertoire [56] as well as for clones from DENV NS1 immunized mice (Fig. 5 G).

Discussion

The humoral immune response to ZIKV infection in humans is characterized by early appearance of antibodies to structural proteins of the viral capsid followed by a later increase

in antibodies to the non-structural protein NS1 [13, 14]. Here, we found that the humoral immune response of immunocompetent BALB/c mice to ZIKV infection follows a similar pattern. The BALB/c antibody response is characterized by early emergence of envelope-specific IgG, including EDIII-specific and neutralizing antibodies, followed by a delayed response dominated by antibodies to NS1. The delayed response to NS1 may be a consequence of its absence from the viral particle, possibly explaining the initial dominance of anti-envelope antibodies. Only after productive ZIKV infection do cells start producing and secreting large amounts of NS1, which then accumulates in bodily fluids and on the surface of infected cells. NS1 circulates in blood, and has been implicated both in damage to endothelial cells and in immune evasion through inhibition of the complement cascade. Of note, antibodies to NS1 have been shown to be protective against dengue disease, and immunization with NS1 has been considered as a possible immunotherapeutic strategy.

Antibodies to DENV NS1 have also been implicated in pathological autoreactivity in humans. From that perspective, it is interesting to note that autoreactivity towards self-antigens present in different tissue or cell extracts was observed in the humoral response of BALB/c mice to ZIKV infection. The presence of autoreactive antibodies in viral diseases is not an uncommon finding and is often attributed to non-specific polyclonal B cell activation. Autoreactive B cells could be stimulated in a T-independent manner, via simultaneous TLR7 and BCR signaling both in GCs and in extrafollicular foci [57-60]. However, polyclonal B lymphocyte activation is an acute phase phenomenon that subsides with clearance of the virus. Here, by contrast, we found that self-reactivity was sustained and even augmented in late time points after infection, long after ZIKV has been eliminated. Interestingly, the presence of NS1-specific antibodies was also long-lasting and correlated well with the kinetics of appearance and maintenance of autoreactive antibodies in BALB/c mice. The IgG isotype composition of the NS1 specific repertoire was coherent with the sustained IgG anti-NS1 response and with engagement of new clonotypes, since the early IgG2a response is followed by a later emergence of IgG1. At the same time, IgG2a titers still increased up to 50 days after infection. It is still not clear whether the response triggered by the viral antigen is maintained by self-antigens or if the viral antigen is still present at later time points even though the virus was not detected at any time after the first week of infection, as long-term antigen persistence follicular dendritic cells has been well documented [61]. In any case, the kinetics of the NS1 response is unique and differs from that induced by viral surface antigens, progressively dominating the humoral response. The shift from anti-capsid to anti-NS1 response may well be a viral escape strategy, since neutralization is only achieved by antibodies directed to viral surface proteins.

Our analysis of GC B cells in ZIKV infected mice revealed both virus-specific and self-reactive B cells in GCs. Both for NS1 protein and self-antigens, reactivity of antibodies derived

from GC B cells was determined by limiting dilution analysis. At that point in our study, we could not yet determine whether anti-NS1 clonotypes were cross-reactive with self-antigens or not; however the experiments we conducted with single-cell cultures showed that both reactivities could often be attributed to the same cell. The GC response of ZIKV infected animals seems to be of short duration, as we did not find long-lasting GCs in spleen or lymph nodes; however, autoreactive clones were found at all time points investigated. Autoreactivity was also present in NS1-immunized mice. The kinetics of the response to ZIKV NS1 after immunization was similar to the response to DENV NS1, although no self-reactivity was found in the latter case. It is worth noting that anti-ZIKV NS1 do not cross react with DENV NS1, in agreement with the distinct reactivity profiles reported here.

Enrichment for charged amino acids, especially arginine, in CDR-H3 has been described in self-reactive antibodies associated with autoimmune diseases, such as lupus [62]. Under normal circumstances, immunocompetent BALB/c mice are considered to be resistant to production of autoantibodies [63]. This is in part due to the low prevalence (around 5%) of arginine in the CDR-H3 region of the BCRs of mature recirculating B cells in BALB/c mice [56]. Half of the arginines in CDR-H3 regions of immature B cells in BALB/c mice derive from N-additions and half from germline DH sequences [64]. Here, we found an enrichment for charged amino acids, including arginine, in CDR-H3 of GC B cell receptors after ZIKV NS1 immunization, as compared to DENV NS1. Interestingly, one particular clone found at high frequency among GC B cells at day 14 after immunization with ZIKV utilized the D gene segment DSP2.11 (D2-14), the only one to encode arginine in the germline sequence in reading frame 1 [64]. Notably, a marked glycine enrichment in CDR-H3 was also observed, which might contribute to maintaining the overall average hydrophobicity close to neutrality.

VH sequencing of clones isolated from GC of ZIKV NS1 or DENV NS1-immunized mice showed similar usage of VH genes, except that VH mutation numbers were lower among clones found more frequently in both cases, possibly indicating B cell clonotypes undergoing stronger antigen-driven selection. We speculate that this could be due to the availability, in the pre-immune repertoire, of B cells able to bind to ZIKV NS1 protein with enough affinity to differentiate rapidly into plasma cells before accumulating many mutations. As recently shown by Burnett and colleagues, selection in GCs is skewed towards lower affinity for self-antigens prior to increasing affinity to foreign antigens [65]. In this context, it is possible that anti-ZIKV NS1 clonotypes could generate plasma cells before enough mutations are acquired to lower self-antigen affinity. While it is known that plasma cell differentiation in GCs is dependent on high BCR affinity, the mechanisms through which the affinity threshold for differentiation is set are unclear [66, 67].

Coupling sequence analysis to binding assays, we found that NS1-specific B cells had similar numbers of VH mutations (higher than those of non-specific clones), regardless of

whether they were self-reactive or not. By contrast, self-reactive B cells that did not bind to ZIKV NS1 protein were the least mutated of all, and were also not detectably expanded (Figure 6E). This data suggest the presence of antigen-driven selection in spite of self-reactivity, although, among NS1-specific cells, self-reactive cells seem slightly disfavored as compared to non-self-reactive ones. For instance, the glycine enriched CDR-H3 ARGGGFDGFAY was a present in a highly expanded clone of which the least mutated variant was autoreactive, and multiple mutated variants, such as ARGGGYDGFAY, lost self-reactivity. The autoreactive clone ARGTLY**A**MDY, on the other hand, was found in both a more mutated non-autoreactive form ARGTLY**T**MDY as well as in a more mutated autoreactive form ARGTLY**S**MDY (Table S1). These observations suggest that GC B cell clones in ZIKV NS1 immunization tend to be closer to germline than in DENV NS1 immunization, an intriguing finding that needs further confirmation.

In conclusion, we show here, for the first time, that anti-ZIKV NS1 GC B cells can cross-react with self-antigens, suggesting an mimicry between ZIKV NS1 and self. The possible similarity of ZIKV NS1 protein to self-antigens could explain the sustained progression of the humoral immune response we observed in infected mice, which display similar kinetics of anti-NS1 and self-reactive antibodies in serum. Finally, of note, autoreactive clones that do not react with NS1 were also documented in GC, raising the possibility of a true breakage of self-tolerance upon viral infection.

Material and methods

Mice and treatments

BALB/c adult female mice, aged 6 to 8 weeks, were obtained from NAL-UFF, LAT-UFRJ or The Jackson Laboratory. Mice were kept in a 12h light/dark cycle with ad libitum access to food and water. Mice were infected with 10^6-10^7 PFU of ZIKV PE243 [36] i.v. and blood samples were collected on days 2, 7, 14, 21, 28, 35, 42, 50 or 60, as indicated for each experiment. ZIKV strain PE243 (Brazil/South America, gene bank accession no. KX197192) was propagated and titrated in Vero cells and UV-inactivated as previously described [36]. All animal procedures were approved by the Institutional Animal Care and Use Committee of the Centro de Ciências da Saúde da Universidade Federal do Rio de Janeiro and the Rockefeller University.

ELISA for immunoglobulin quantification

Total IgG and IgM concentration in serum and cell culture supernatants were determined by ELISA as previously described in [68] using anti-mouse IgM and IgG-specific reagents (Southern Biotechnology). Briefly, 96 well plates (Costar) were incubated with anti-IgM or anti-IgG capturing antibody at 1ug/ml (Southern Biotech) and incubated at 4°C for 18h. Then, after

1h of blocking (PBS-1%BSA), serum samples and culture supernatants were diluted in PBS-BSA 1% by serial dilution starting at 1:40 for serum and undiluted for supernatants. Standard curves of polyclonal IgM or IgG were obtained by serial dilution 3-fold for IgM and 5-fold for IgG, starting at 1ug/mL for supernatants and 2ug/mL for serum samples. Secondary antibodies conjugated to HRP (Southern Biotech) were diluted 1:2000 for IgM and 1:8000 for IgG in PBS-BSA 1%. After wash with PBS, reactions were developed with TMB substrate solution (Sigma). The reaction was stopped with HCL 1N.

ELISA for antigen-specific immunoglobulin detection

ELISAs to determine serum levels of anti-VLPs, anti-EDIII and anti-NS1 antibodies as well as specificity of IgG in B cell culture supernatants were performed as previously described [69]. Briefly, 96 well plates (Costar) were coated with peptide (EDIII) (10 µg/ml) or protein (1µg/ml) diluted in PBS and incubated at 4°C for 18h. Serum samples were diluted following serial dilution 1:3 for IgM and IgG starting with 1:40 in the first well. ZIKV and DENV EDIII recombinant proteins were kindly provided by Dr. Orlando Ferreira, IB, UFRJ. VLPs were produced and purified as previously described [37]. ZIKV and DENV NS1 proteins were produced and purified as reported previously.

Immunoblot

BALB/c tissues (brain and skeletal muscle) were dissociated by Polytron homogenizer (4000 rpm) in homogenizing buffer (Tris-HCl 0,5M pH 6,8, SDS 10%, Mili-Q water) as described by Haury et al.[48]. Tissue extracts were fractioned by electrophoresis in 10% polyacrylamide gel under denaturing conditions, at 50mA until 6cm of migration. Proteins were transferred from the gel to a nitrocellulose membrane by a semi-dry electro transfer (Semi-Dry Electroblotter B) for 60 minutes at 0,8mA/cm². After transfer, the membrane was kept in 50mL of PBS/Tween 20 (BioRad) at 0,2% vol/vol shaking for 18 hours at room temperature.

Incubation of the membrane with cell culture supernatants or serum samples was performed in a Miniblot System Cassette (Immunetics Inc.) which allows the simultaneous incubation of 28 different samples in separated channels. Supernatant samples were diluted 1:2 and serum samples were diluted 1:100. After wash, membranes were incubated with secondary antibodies conjugated to alkaline phosphatase anti-IgM or anti-IgG diluted 1:2000 (rabbit anti-mouse IgM, Jackson ImmunoResearch, goat anti-mouse IgG, SouthernBiotech). Substrate NBT/BCIP (Promega) was added after wash. Reaction was developed shaking at room temperature and stopped with Milli-Q water. Colloidal gold staining was performed after scanning membranes.

Flow cytometry and cell sorting

Cells were harvested from spleen, peritoneal cavity and popliteal lymph nodes for flow cytometry and cell sorting. Splenocytes were homogenized with complete RPMI 1640 medium (GIBCO), followed by red blood cell lysis in 1 mL of ACK lysing buffer (GIBCO) for 1 min on ice. Single cell suspensions were prepared from the peritoneal cavity lavage with 5ml of complete RPMI 1640 medium (GIBCO). Popliteal lymph nodes were homogenized with complete RPMI 1640 medium (GIBCO). Cells were washed and resuspended in an appropriate volume for counting and staining. Cells were stained with the following monoclonal Abs conjugated to fluorochromes: anti-B220, CD38, CD138, GL-7, CD21, CD23, CD93 (AA4.1), CD11b, CD5, IgM and CD44 (eBioscience) for 30 minutes at 4°C in FACS staining buffer (PBS 1x with 5% FCS). Analysis and cell sort were then performed on a MoFlo instrument (Dako-Cytomation). B cell populations were defined as follows: GC (B220+ CD138- CD38lo/- GL-7+), FO (B220+ CD138- CD21+ CD23-) and MZ (B220+ CD138- CD21- CD23+), B1-a (B220int/low CD5+), B1-b (B220int/low CD5-) and B-2 (B220high CD5-). Cells were collected directly in sterile tubes containing supplemented OptiMEM (GIBCO) for cell culture.

GC B cell culture in limiting dilution assay (LDA)

Decreasing number of GC B cells were cultured in 250 µl of OptiMEM (GIBCO) supplemented with 10% heat-inactivated FBS (GIBCO), 2 mM L-glutamine, 1 mM sodium pyruvate, 50 µM 2-ME, 100 U penicillin, and 100 µg/ml streptomycin. All cultures were performed in 96-well flat bottom plates containing $3x10^3$ NB40L feeder cells/well as previously described protocol with minor modifications [70]. GC B cells were added starting from 3000 cells/well to 1 cell/well through 3-fold dilution steps in the presence of 30 µg/ml of LPS (Salmonella typhimurium, Sigma-Aldrich) and 2 ng/ml of IL-21 (Peprotech). After 7 days, cultures were screened by ELISA to determine the frequency of IgG secreting GC B cells according to the Poisson distribution [71, 72].

Single GC B cell cultures

Single GC B cells were sorted into 96-well round-bottom plates containing $3x10^3$ NB21 cells/well as previously described with minor modifications, mostly not adding IL-4 [51]. Supernatants were collected after 7 days of culture and cells were frozen in TCL lysis buffer supplemented with 1%β-mercaptoethanol for *Igh* sequencing.

Igh sequencing

Single GC B cells from popliteal lymph nodes of Balb/c mice immunized with ZIKV or DENV NS1 proteins were sorted into 96-well PCR plates directly or after 7 days in culture. Plates contained 5 µl of TCL lysis buffer (Qiagen) supplemented with 1%β-mercaptoethanol. RNA extraction was performed using SPRI bead as described in [66]. RNA was reverse transcribed into cDNA using an oligo (dT) primer. *Igh* transcripts were amplified as described

in [73]. PCR products were barcoded and sequenced utilizing MiSeq (Illumina) Nano kit v.2 as described in [74].

Paired-end sequences were assembled with PandaSeq [75] and processed with the FASTX toolkit. The resulting demultiplexed and collapsed reads were assigned to wells according to barcodes. High-count sequences for every single cell/well were analyzed. Ig heavy chains were aligned to both IMGT [76] and Vbase2 [77] databases, in case of discrepancy IgBLAST was used. VH mutation analyses were restricted to cells with productively rearranged *Igh* genes, as described in [74]. CDR-H3 analyses were performed as described in [78]. Average hydrophobicity of CDR-H3 was calculated as previously described in [79]. Functional rearrangements were grouped by clones defined by identical VH and JH segment and identical CDR-H3 length and amino acid sequence.

Statistical analyses

Statistical analyses were performed using GraphPadPrism 7.0 software. Tests were chosen according to the type of variable and indicated in each result. Results with $p > 0.05$ were considered significant.

Principal component analysis (PCA) was performed to compare the repertoires globally. Reactivity sections were defined and signal intensities across the sections were quantified and analyzed as described in [80].

Acknowledgements

We thank Dr. Orlando Ferreira for kindly providing ZIKV and DENV EDIII recombinant proteins. We thank Dr. M. Bozza for helpful discussions and suggestions. This work was supported by the Brazilian research funding agencies Fundação de Amparo à Pesquisa do Estado do Rio de Janeiro (FAPERJ), Conselho Nacional de Desenvolvimento Científico e Tecnológico (CNPq), Coordenação de Aperfeiçoamento de Pessoal de Nível Superior (CAPES). CBC was supported by CNPq (PhD fellowship), and CAPES (PDSE 88881.132337/2016-01 and Projeto de pesquisa 1759/2014 - Biocomputacional - process number 23038.004628/2014-66).

References

1. Hunziker, L., et al., *Hypergammaglobulinemia and autoantibody induction mechanisms in viral infections.* Nat Immunol, 2003. **4**(4): p. 343-9.
2. Root-Bernstein, R. and D. Fairweather, *Complexities in the relationship between infection and autoimmunity.* Curr Allergy Asthma Rep, 2014. **14**(1): p. 407.
3. Balakrishnan, T., et al., *Dengue virus activates polyreactive, natural IgG B cells after primary and secondary infection.* PLoS One, 2011. **6**(12): p. e29430.

4. Barbi, L., et al., *Prevalence of Guillain-Barré syndrome among Zika virus infected cases: a systematic review and meta-analysis.* Braz J Infect Dis, 2018. **22**(2): p. 137-141.
5. de Oliveira, W.K., et al., *Infection-related microcephaly after the 2015 and 2016 Zika virus outbreaks in Brazil: a surveillance-based analysis.* Lancet, 2017. **390**(10097): p. 861-870.
6. Lardone, R.D., et al., *Anti-GM1 IgG antibodies in Guillain-Barré syndrome: fine specificity is associated with disease severity.* J Neurol Neurosurg Psychiatry, 2010. **81**(6): p. 629-33.
7. Akey, D.L., et al., *Flavivirus NS1 structures reveal surfaces for associations with membranes and the immune system.* Science, 2014. **343**(6173): p. 881-5.
8. Brown, W.C., et al., *Extended surface for membrane association in Zika virus NS1 structure.* Nat Struct Mol Biol, 2016. **23**(9): p. 865-7.
9. Cox, B.D., R.A. Stanton, and R.F. Schinazi, *Predicting Zika virus structural biology: Challenges and opportunities for intervention.* Antivir Chem Chemother, 2015. **24**(3-4): p. 118-26.
10. Young, P.R., et al., *An antigen capture enzyme-linked immunosorbent assay reveals high levels of the dengue virus protein NS1 in the sera of infected patients.* J Clin Microbiol, 2000. **38**(3): p. 1053-7.
11. Hilgenfeld, R., *Zika virus NS1, a pathogenicity factor with many faces.* EMBO J, 2016. **35**(24): p. 2631-2633.
12. Freire, M.C.L.C., et al., *Mapping Putative B-Cell Zika Virus NS1 Epitopes Provides Molecular Basis for Anti-NS1 Antibody Discrimination between Zika and Dengue Viruses.* ACS Omega, 2017. **2**(7): p. 3913-3920.
13. Gao, X., et al., *Delayed and highly specific antibody response to nonstructural protein 1 (NS1) revealed during natural human ZIKV infection by NS1-based capture ELISA.* BMC Infect Dis, 2018. **18**(1): p. 275.
14. Stettler, K., et al., *Specificity, cross-reactivity, and function of antibodies elicited by Zika virus infection.* Science, 2016. **353**(6301): p. 823-6.
15. Gonçalves, A.J., et al., *Cooperation between CD4+ T Cells and Humoral Immunity Is Critical for Protection against Dengue Using a DNA Vaccine Based on the NS1 Antigen.* PLoS Negl Trop Dis, 2015. **9**(12): p. e0004277.
16. Richner, J.M., et al., *Vaccine Mediated Protection Against Zika Virus-Induced Congenital Disease.* Cell, 2017. **170**(2): p. 273-283.e12.
17. Bailey, M.J., et al., *Antibodies Elicited by an NS1-Based Vaccine Protect Mice against Zika Virus.* mBio, 2019. **10**(2).
18. Chuang, Y.C., et al., *Dengue Virus Nonstructural Protein 1-Induced Antibodies Cross-React with Human Plasminogen and Enhance Its Activation.* J Immunol, 2016. **196**(3): p. 1218-26.
19. Lee, P.X., et al., *Relative contribution of nonstructural protein 1 in dengue pathogenesis.* J Exp Med, 2020. **217**(9).
20. Beatty, P.R., et al., *Dengue virus NS1 triggers endothelial permeability and vascular leak that is prevented by NS1 vaccination.* Sci Transl Med, 2015. **7**(304): p. 304ra141.
21. Falconar, A.K., *The dengue virus nonstructural-1 protein (NS1) generates antibodies to common epitopes on human blood clotting, integrin/adhesin proteins and binds to human endothelial cells: potential implications in haemorrhagic fever pathogenesis.* Arch Virol, 1997. **142**(5): p. 897-916.

22. Reyes-Sandoval, A. and J.E. Ludert, *The Dual Role of the Antibody Response Against the Flavivirus Non-structural Protein 1 (NS1) in Protection and Immuno-Pathogenesis.* Front Immunol, 2019. **10**: p. 1651.
23. Zellweger, R.M., T.R. Prestwood, and S. Shresta, *Enhanced infection of liver sinusoidal endothelial cells in a mouse model of antibody-induced severe dengue disease.* Cell Host Microbe, 2010. **7**(2): p. 128-39.
24. Lazear, H.M., et al., *A Mouse Model of Zika Virus Pathogenesis.* Cell Host Microbe, 2016. **19**(5): p. 720-30.
25. Yauch, L.E. and S. Shresta, *Mouse models of dengue virus infection and disease.* Antiviral Res, 2008. **80**(2): p. 87-93.
26. Bardina, S.V., et al., *Enhancement of Zika virus pathogenesis by preexisting antiflavivirus immunity.* Science, 2017. **356**(6334): p. 175-180.
27. Demengeot, J., et al., *B lymphocyte sensitivity to IgM receptor ligation is independent of maturation stage and locally determined by macrophage-derived IFN-beta.* Int Immunol, 1997. **9**(11): p. 1677-85.
28. Kiefer, K., et al., *Role of type I interferons in the activation of autoreactive B cells.* Immunol Cell Biol, 2012. **90**(5): p. 498-504.
29. Lucas, C.G.O., et al., *Critical role of CD4+ T cells and IFNγ signaling in antibody-mediated resistance to Zika virus infection.* Nature Communications, 2018. **9**(1): p. 3136.
30. Hassert, M., et al., *CD4+T cells mediate protection against Zika associated severe disease in a mouse model of infection.* PLoS Pathog, 2018. **14**(9): p. e1007237.
31. Elong Ngono, A., et al., *CD4+ T cells promote humoral immunity and viral control during Zika virus infection.* PLoS Pathog, 2019. **15**(1): p. e1007474.
32. Winkler, C.W., et al., *Adaptive Immune Responses to Zika Virus Are Important for Controlling Virus Infection and Preventing Infection in Brain and Testes.* J Immunol, 2017. **198**(9): p. 3526-3535.
33. Pardy, R.D., et al., *Analysis of the T Cell Response to Zika Virus and Identification of a Novel CD8+ T Cell Epitope in Immunocompetent Mice.* PLoS Pathog, 2017. **13**(2): p. e1006184.
34. Huang, H., et al., *CD8(+) T Cell Immune Response in Immunocompetent Mice during Zika Virus Infection.* J Virol, 2017. **91**(22).
35. Dai, L., et al., *Structures of the Zika Virus Envelope Protein and Its Complex with a Flavivirus Broadly Protective Antibody.* Cell Host Microbe, 2016. **19**(5): p. 696-704.
36. Coelho, S.V.A., et al., *Development of standard methods for Zika virus propagation, titration, and purification.* J Virol Methods, 2017. **246**: p. 65-74.
37. Alvim, R.G.F., I. Itabaiana, and L.R. Castilho, *Zika virus-like particles (VLPs): Stable cell lines and continuous perfusion processes as a new potential vaccine manufacturing platform.* Vaccine, 2019. **37**(47): p. 6970-6977.
38. Beasley, D.W. and A.D. Barrett, *Identification of neutralizing epitopes within structural domain III of the West Nile virus envelope protein.* J Virol, 2002. **76**(24): p. 13097-100.
39. Oliphant, T., et al., *Development of a humanized monoclonal antibody with therapeutic potential against West Nile virus.* Nat Med, 2005. **11**(5): p. 522-30.
40. Shrestha, B., et al., *The development of therapeutic antibodies that neutralize homologous and heterologous genotypes of dengue virus type 1.* PLoS Pathog, 2010. **6**(4): p. e1000823.

41. Watterson, D., N. Modhiran, and P.R. Young, *The many faces of the flavivirus NS1 protein offer a multitude of options for inhibitor design.* Antiviral Res, 2016. **130**: p. 7-18.
42. Coutelier, J.P., et al., *IgG2a restriction of murine antibodies elicited by viral infections.* J Exp Med, 1987. **165**(1): p. 64-9.
43. Wang, J., et al., *A Human Bi-specific Antibody against Zika Virus with High Therapeutic Potential.* Cell, 2017. **171**(1): p. 229-241.e15.
44. Victora, G.D., et al., *Mother-child immunological interactions in early life affect long-term humoral autoreactivity to heat shock protein 60 at age 18 years.* J Autoimmun, 2007. **29**(1): p. 38-43.
45. Füst, G., et al., *Antibodies against heat shock proteins and cholesterol in HIV infection.* Mol Immunol, 2005. **42**(1): p. 79-85.
46. Quintana, F.J. and I.R. Cohen, *The HSP60 immune system network.* Trends Immunol, 2011. **32**(2): p. 89-95.
47. Nobrega, A., et al., *Global analysis of antibody repertoires. II. Evidence for specificity, self-selection and the immunological "homunculus" of antibodies in normal serum.* Eur J Immunol, 1993. **23**(11): p. 2851-9.
48. Haury, M., et al., *Global analysis of antibody repertoires. 1. An immunoblot method for the quantitative screening of a large number of reactivities.* Scand J Immunol, 1994. **39**(1): p. 79-87.
49. Wardemann, H., et al., *Predominant autoantibody production by early human B cell precursors.* Science, 2003. **301**(5638): p. 1374-7.
50. Victora, G.D. and M.C. Nussenzweig, *Germinal centers.* Annu Rev Immunol, 2012. **30**: p. 429-57.
51. Kuraoka, M., et al., *Complex Antigens Drive Permissive Clonal Selection in Germinal Centers.* Immunity, 2016. **44**(3): p. 542-552.
52. Nobrega, A., et al., *Functional diversity and clonal frequencies of reactivity in the available antibody repertoire.* Eur J Immunol, 1998. **28**(4): p. 1204-15.
53. Vale, A.M., et al., *A rapid and quantitative method for the evaluation of V gene usage, specificities and the clonal size of B cell repertoires.* J Immunol Methods, 2012. **376**(1-2): p. 143-9.
54. Radic, M.Z., et al., *B lymphocytes may escape tolerance by revising their antigen receptors.* J Exp Med, 1993. **177**(4): p. 1165-73.
55. Radic, M.Z. and M. Weigert, *Genetic and structural evidence for antigen selection of anti-DNA antibodies.* Annu Rev Immunol, 1994. **12**: p. 487-520.
56. Ivanov, I.I., et al., *Development of the expressed Ig CDR-H3 repertoire is marked by focusing of constraints in length, amino acid use, and charge that are first established in early B cell progenitors.* J Immunol, 2005. **174**(12): p. 7773-80.
57. Akkaya, M., et al., *Toll-like receptor 9 antagonizes antibody affinity maturation.* Nat Immunol, 2018. **19**(3): p. 255-266.
58. Bessa, J., M. Kopf, and M.F. Bachmann, *Cutting edge: IL-21 and TLR signaling regulate germinal center responses in a B cell-intrinsic manner.* J Immunol, 2010. **184**(9): p. 4615-9.
59. Das, A., et al., *Follicular Dendritic Cell Activation by TLR Ligands Promotes Autoreactive B Cell Responses.* Immunity, 2017. **46**(1): p. 106-119.
60. Degn, S.E., et al., *Clonal Evolution of Autoreactive Germinal Centers.* Cell, 2017. **170**(5): p. 913-926.e19.

61. Heesters, B.A., R.C. Myers, and M.C. Carroll, *Follicular dendritic cells: dynamic antigen libraries.* Nat Rev Immunol, 2014. **14**(7): p. 495-504.
62. Radic, M.Z. and M. Weigert, *Origins of anti-DNA antibodies and their implications for B-cell tolerance.* Ann N Y Acad Sci, 1995. **764**: p. 384-96.
63. Sekiguchi, D.R., et al., *Development and selection of edited B cells in B6.56R mice.* J Immunol, 2006. **176**(11): p. 6879-87.
64. Silva-Sanchez, A., et al., *Violation of an evolutionarily conserved immunoglobulin diversity gene sequence preference promotes production of dsDNA-specific IgG antibodies.* PLoS One, 2015. **10**(2): p. e0118171.
65. Burnett, D.L., et al., *Germinal center antibody mutation trajectories are determined by rapid self/foreign discrimination.* Science, 2018. **360**(6385): p. 223-226.
66. Tas, J.M., et al., *Visualizing antibody affinity maturation in germinal centers.* Science, 2016. **351**(6277): p. 1048-54.
67. Viant, C., et al., *Antibody Affinity Shapes the Choice between Memory and Germinal Center B Cell Fates.* Cell, 2020. **183**(5): p. 1298-1311.e11.
68. Vale, A.M., et al., *Genetic control of the B cell response to LPS: opposing effects in peritoneal versus splenic B cell populations.* Immunogenetics, 2010. **62**(1): p. 41-8.
69. Lucas, C.G.O., et al., *Critical role of CD4.* Nat Commun, 2018. **9**(1): p. 3136.
70. Nojima, T., et al., *In-vitro derived germinal centre B cells differentially generate memory B or plasma cells in vivo.* Nat Commun, 2011. **2**: p. 465.
71. Andersson, J., et al., *Clonal growth and maturation to immunoglobulin secretion in vitro of every growth-inducible B lymphocyte.* Cell, 1977. **10**(1): p. 27-34.
72. Taswell, C., *Limiting dilution assays for the determination of immunocompetent cell frequencies. I. Data analysis.* J Immunol, 1981. **126**(4): p. 1614-9.
73. Tiller, T., C.E. Busse, and H. Wardemann, *Cloning and expression of murine Ig genes from single B cells.* J Immunol Methods, 2009. **350**(1-2): p. 183-93.
74. Mesin, L., et al., *Restricted Clonality and Limited Germinal Center Reentry Characterize Memory B Cell Reactivation by Boosting.* Cell, 2020. **180**(1): p. 92-106.e11.
75. Masella, A.P., et al., *PANDAseq: paired-end assembler for illumina sequences.* BMC Bioinformatics, 2012. **13**: p. 31.
76. Lefranc, M.P., et al., *IMGT, the international ImMunoGeneTics information system.* Nucleic Acids Res, 2009. **37**(Database issue): p. D1006-12.
77. Retter, I., et al., *VBASE2, an integrative V gene database.* Nucleic Acids Res, 2005. **33**(Database issue): p. D671-4.
78. Ivanov, II, et al., *Development of the expressed Ig CDR-H3 repertoire is marked by focusing of constraints in length, amino acid use, and charge that are first established in early B cell progenitors.* J Immunol, 2005. **174**(12): p. 7773-80.
79. Kyte, J. and R.F. Doolittle, *A simple method for displaying the hydropathic character of a protein.* J Mol Biol, 1982. **157**(1): p. 105-32.
80. Mouthon, L., et al., *Invariance and restriction toward a limited set of self-antigens characterize neonatal IgM antibody repertoires and prevail in autoreactive repertoires of healthy adults.* Proc Natl Acad Sci U S A, 1995. **92**(9): p. 3839-43.

Figures and Legends

Figure 1

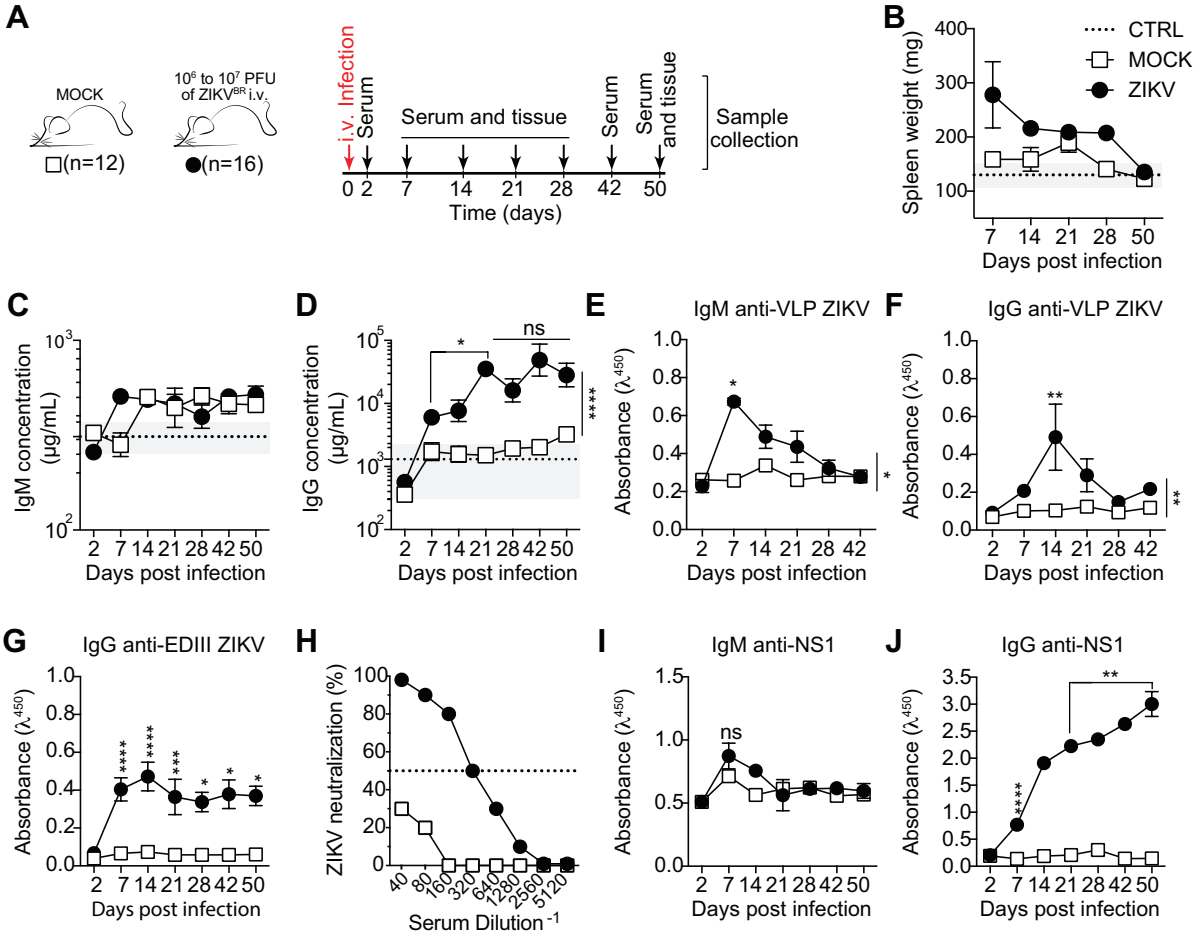

Figure 1. Characterization of infection in immunocompetent BALB/c mice. (A) Experimental design indicating the time points of serum samples and lymphoid tissue collections. **(B)** Spleen weight measured at the time of collection, as indicated. Total serum IgM **(C)** and IgG **(D)** from infected (ZIKV) and control (MOCK) mice, measured by ELISA. (**E-G**) Levels of IgM and IgG specific for viral surface antigens were measured by ELISA (1:120 dilution) utilizing VLPs and recombinant domain III of ZIKV envelope protein (EDIII). (**H**) Plaque reduction neutralization test was performed in pooled sera from control (MOCK) and infected (ZIKV) mice at 14 days post-infection. (**I-J**) Levels of IgM (**I**) and IgG (**J**) specific for NS1 protein were measured by ELISA (1:120 dilution) utilizing recombinant ZIKV NS1. (n=10 mice per group. Representative of two independent experiments). ns = not significant; *p<0,05; **p<0,01; ***p<0,001; ****p<0,0001.

Figure 2

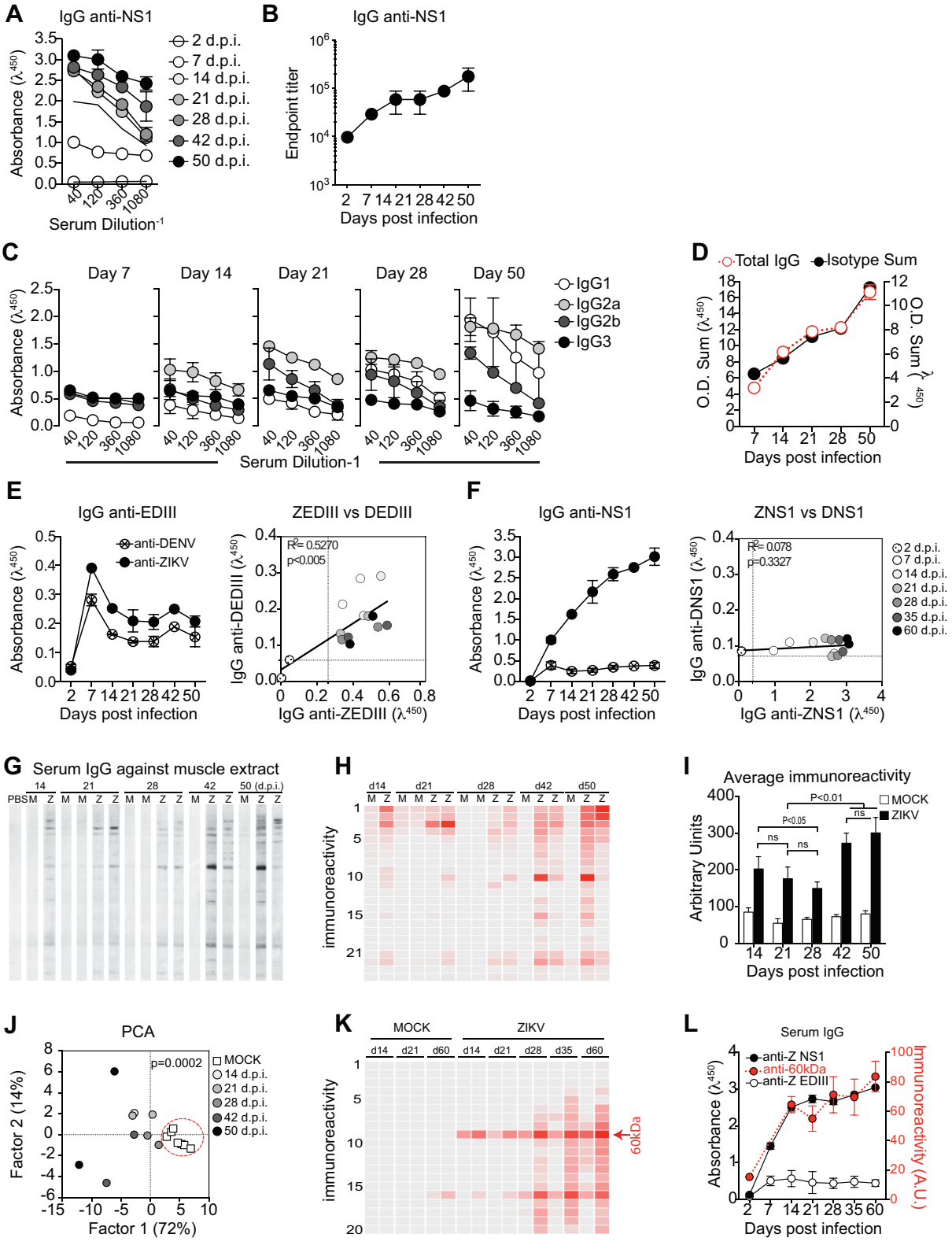

Figure 2. Humoral immune response to NS1 during ZIKV infection correlates with autoreactive antibodies. (A) Binding of serum IgG to ZIKV NS1 protein during infection detected by ELISA. **(B)** Endpoint titer of serum IgG specific to ZIKV NS1 protein during infection. **(C)** NS1-specific serum IgG isotypes during experimental infection were detected by

ELISA. **(D)** Total NS1 specific IgG on serum corresponds to the sum of IgG isotypes, present in distinct proportions after infection. **(E-F)** Sera from ZIKV infected mice (1:120 dilution) were tested by ELISA for binding to ZIKV and DENV antigens EDIII (E) and NS1 (F). Correlation coefficients show cross-reactivity of EDIII–specific IgG but not of NS1-specific IgG. **(G)** Self-reactivities present in serum IgG (diluted 1:100) from control (M) and infected (Z) mice using muscle extract from Balb/c mice as source of self-antigens. **(H)** Intensity of bands was quantified and plotted as a heat map. **(I)**Total immunoreactivity (sum of all bands intensities) present in the sera of infected (ZIKV) and control (MOCK) mice for each time point after infection. **(J)** Principal component analysis (PCA) of all self-reactivities at all time points. Red circle indicates the segregation of the control group. **(K)** Intensity of reactivities present in serum IgG (diluted 1:100) from control (MOCK), UV-ZIKV immunized mice (iZIKV) and infected mice (ZIKV) using HEp-2 cells extract as source of self-antigens. **(L)** Intensity of the reactivity to a selected 60 kDa self-antigen throughout time after infection correlates with levels of serum IgG specific to ZIKV NS1 protein but not with levels of IgG specific to domain III of ZIKV envelope protein (ZEDIII). ns = not significant.

Figure 3

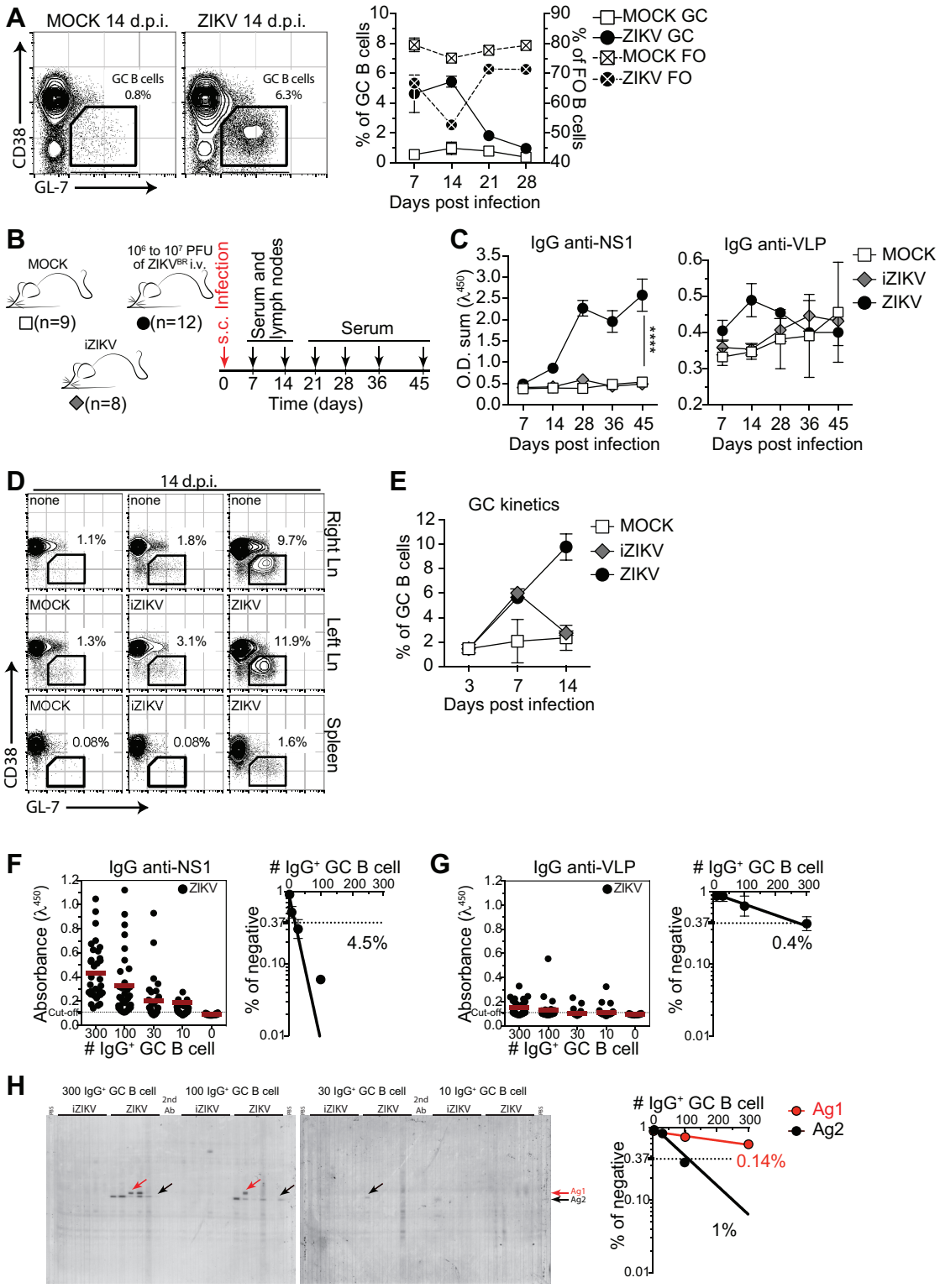

Figure 3. GC B cells produce both virus specific and autoreactive antibodies. (A) GC B cells (CD38$^{lo/-}$ GL-7^{+} gated on B220^{+} CD138^{-}) in the spleen of ZIKV infected mice at 14 days post infection (left). Kinetics of frequency of follicular (FO) and germinal center (GC) B cells after infection is represented in right panel. (**B**) Subcutaneous infection experimental design indicating the time points of serum samples and lymphoid tissue collections from control mice

(MOCK), mice immunized UV-inactivated virus (iZIKV) and infected mice (ZIKV). (**C**) Kinetics of serum IgG specific to ZIKV NS1 and VLPs. OD Sum is the summation of ODs of four serum dilutions (1:40, 1:120, 1:360 and 1:1080). (**D**) Representative plots of GC B cells ($CD38^{lo/-}$ $GL\text{-}7^{+}$ gated on $B220^{+}$ $CD138^{-}$) at day 14 post infection. Mice were injected in the left footpad. (**E**) Kinetics of frequency of germinal center (GC) B cells in left popliteal lymph nodes after infection (ZIKV) or immunization (iZIKV). (**F-H**) GC B cells from popliteal lymph nodes of infected mice were sorted and cultured in decreasing cells numbers/well (300, 100, 30, 10 cells/well). Supernatants were collected on day 7 and screened for IgG secretion by ELISA. Supernatants that revealed the presence of IgG were tested for antigen specificity by ELISA **(F and G)** or immunoblot against mouse brain tissue as source of self-antigens **(H).** Frequencies of IgG^{+} GC B cells that bound NS1 **(F),** VLP **(G)** or self-antigens **(H)** were calculated utilizing Poisson distribution. Self-antigens used for frequency determination are indicated by arrows. Cell culture was performed on a monolayer of gamma-irradiated (20 Gy) NB40L feeder cells (3×10^3 cells/well), LPS (30 µg/mL) and IL-21 (2 ng/mL).

Figure 4

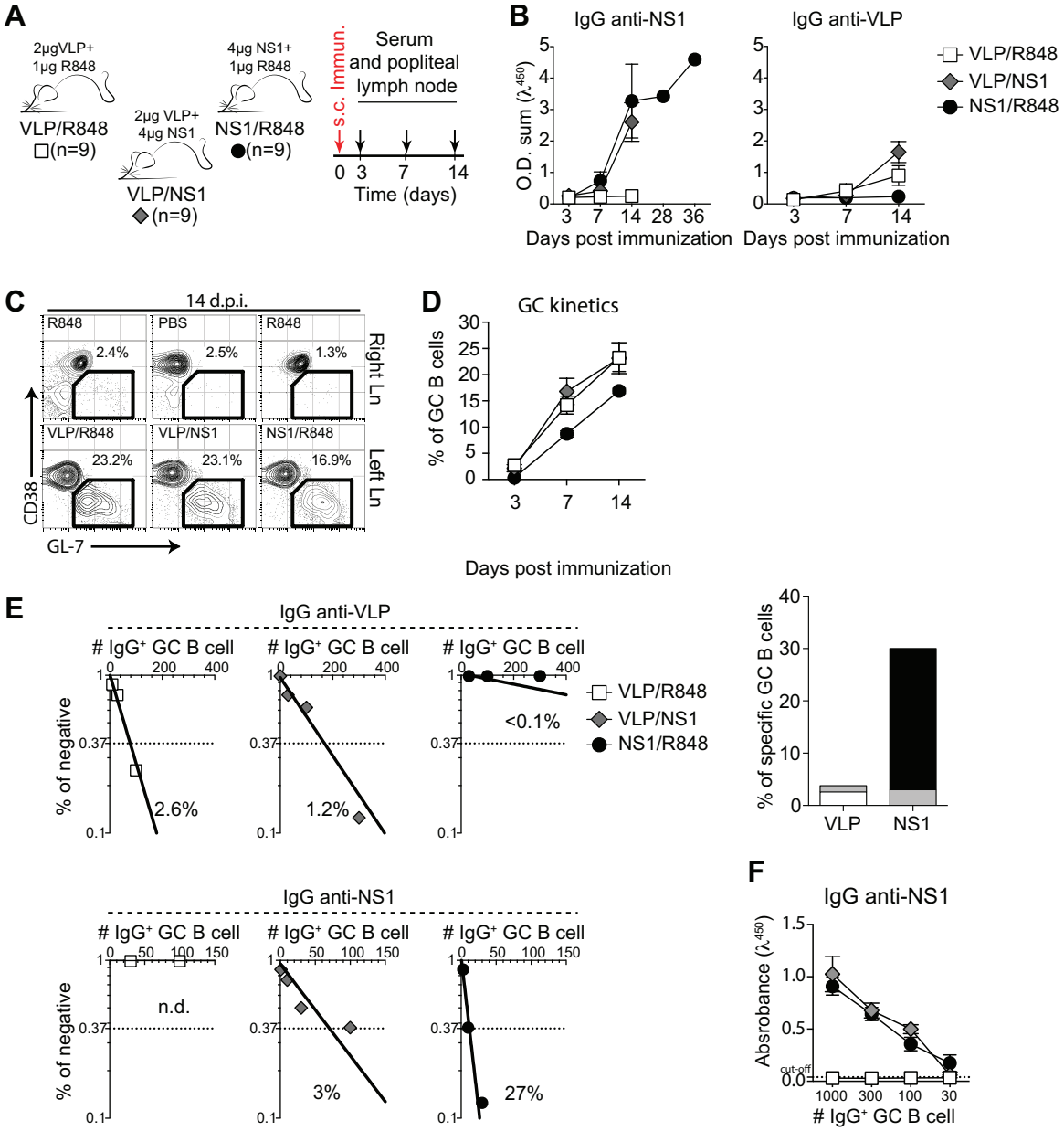

Figure 4. Antigen-specificity of B cells in germinal centers after immunization with ZIKV VLP and NS1. (A) Experimental design indicating the time points of foot pad subcutaneous immunization, serum samples and popliteal lymph nodes collections. **(B)** Kinetics of serum levels of IgG binding to ZIKV NS1 recombinant protein or ZIKV VLP, measured by ELISA. OD Sum is the sum of ODs of four serum dilutions (1:40, 1:120, 1:360 and 1:1080). (**C**) Representative plots of GC B cells ($CD38^{lo/-}$ $GL\text{-}7^{+}$ gated on $B220^{+}$ $CD138^{-}$) at day 14 post immunization. Mice were immunized in the left footpad. (**D**) Kinetics of frequency of germinal center (GC) B cells in left popliteal lymph nodes after immunization with NS1 (2 ug/mouse), VLP (2 ug/mouse) or both (4 ug of NS1 and 2 ug of VLP/mouse). Immunizations were adjuvanted with R848 (1ug/mouse). (**E**) GC B cells from popliteal lymph nodes of immunized mice were sorted and cultured in decreasing cells numbers/well (300, 100, 30, 10 cells/well).

Supernatants were collected on day 7 and screened for IgG secretion by ELISA. Supernatants that revealed the presence of IgG were tested for antigen specificity by ELISA. Frequencies of IgG^+ GC B cells that bound VLP (upper panel) or NS1 (lower panel) were calculated utilizing Poisson distribution and are summarized on the right graph. Cell culture was performed on a monolayer of gamma-irradiated (20 Gy) NB40L feeder cells (3 x 10^3 cells/well), LPS (30 µg/mL) and IL-21 (2 ng/mL). (**F**) OD of IgG^+ supernatants of different cell numbers/well binding to ZIKV NS1, measured by ELISA.

Figure 5

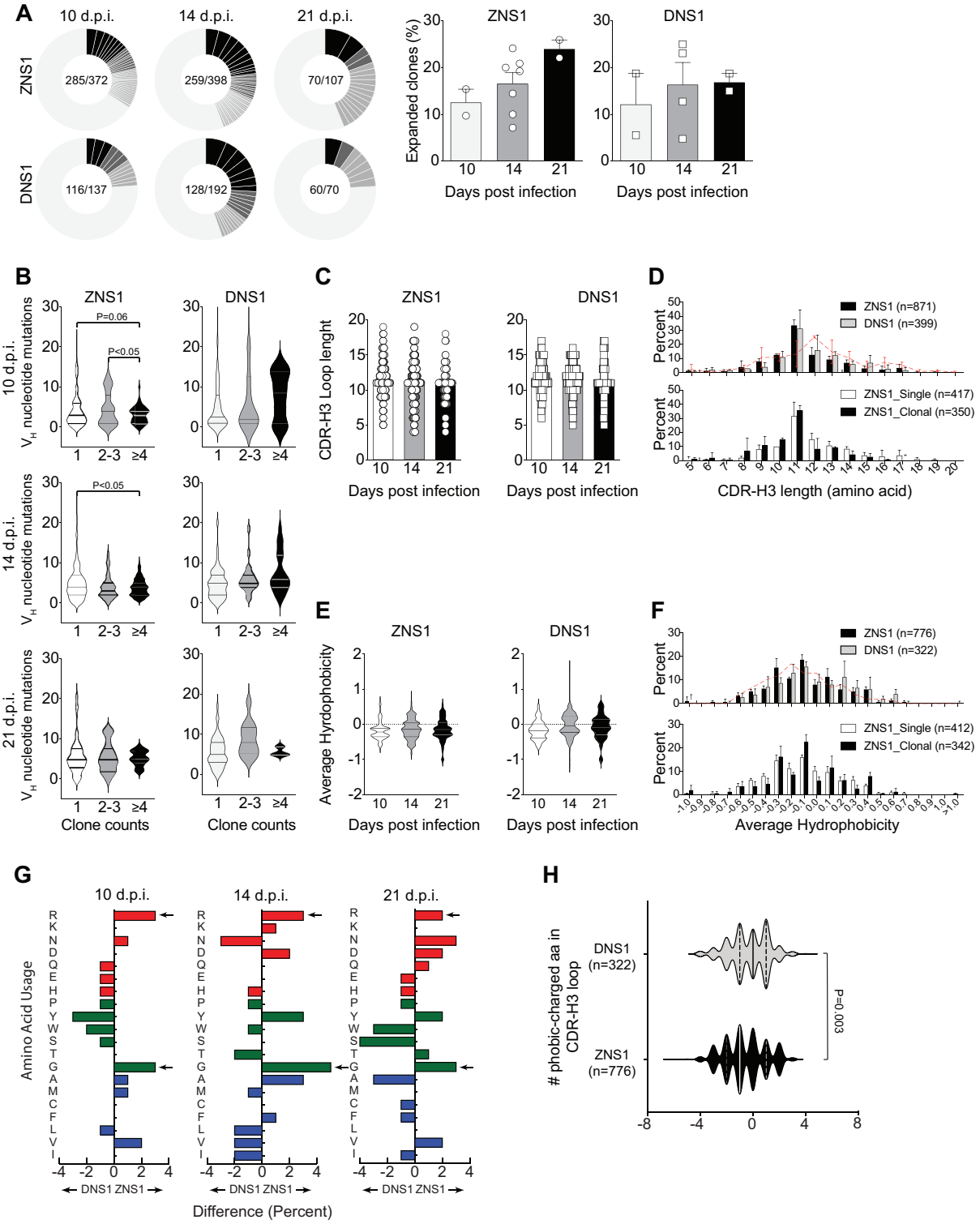

Figure 5. Characterization of B cell repertoire present in GCs after ZIKV NS1 immunization. (A) Single GC B cells from mice immunized s.c. with recombinant ZIKV NS1 or DENV NS1 were sorted at different time points after immunization and *Igh* gene was sequenced. Slices represent clones assigned based on VH usage and CDRH3 sequence. Slice size is proportional to frequency of each clone. Black slices indicate clone counts higher than 4. Dark gray slices indicate clone counts of 3. Lighter gray indicates clone count of 2.

Lightest gray where slices are not delimited represents single clones. **(B)** Number of somatic mutations found in V_H segments from each clone sequenced at different time points in relation to the clone count. **(C)** CDR-H3 loop length variation among all sequences at different time points after immunization with ZIKV NS1 or DENV NS1. **(D)** CDR-H3 loop length distribution comparison among all sequences from mice immunized with ZIKV NS1 or DENV NS1 (upper panel) and comparison between clonal (defined as the sequences with identical rearrangement and CDR-H3 amino acid sequence found more than once in the same lymph node) and single clones from mice immunized with ZIKV NS1 (lower panel). Dashed red line indicates the distribution of CDR-H3 length in follicular B cells from WT BALB/c mice. **(E)** CDR-H3 average hydrophobicity index variation among all sequences at different time points after immunization with ZIKV NS1 or DENV NS1. (**F**) Comparison of CDR-H3 average hydrophobicity index distribution among all sequences from mice immunized with ZIKV NS1 or DENV NS1 (upper panel) and comparison between clonal (defined as the sequences with identical rearrangement and CDR-H3 amino acid sequence found more than once in the same lymph node) and single clones from mice immunized with ZIKV NS1 (lower panel). Dashed red line indicates the distribution of CDR-H3 average hydrophobicity in follicular B cells from WT BALB/c mice. (**G**) Frequency of usage of each amino acid in CDR-H3 after immunization with ZIKV NS1 or DENV NS1 at different time points. Red bars indicate charged amino acids, green bars represent neutral amino acids and blue bars, hydrophobic amino acids. (**H**) Difference in number of hydrophobic and charged amino acids was calculated for each CDR-H3 sequence and distribution was plotted for all sequenced from DENV NS1 immunized mice (gray) and ZIKV NS1 immunized mice (black).

Figure 6

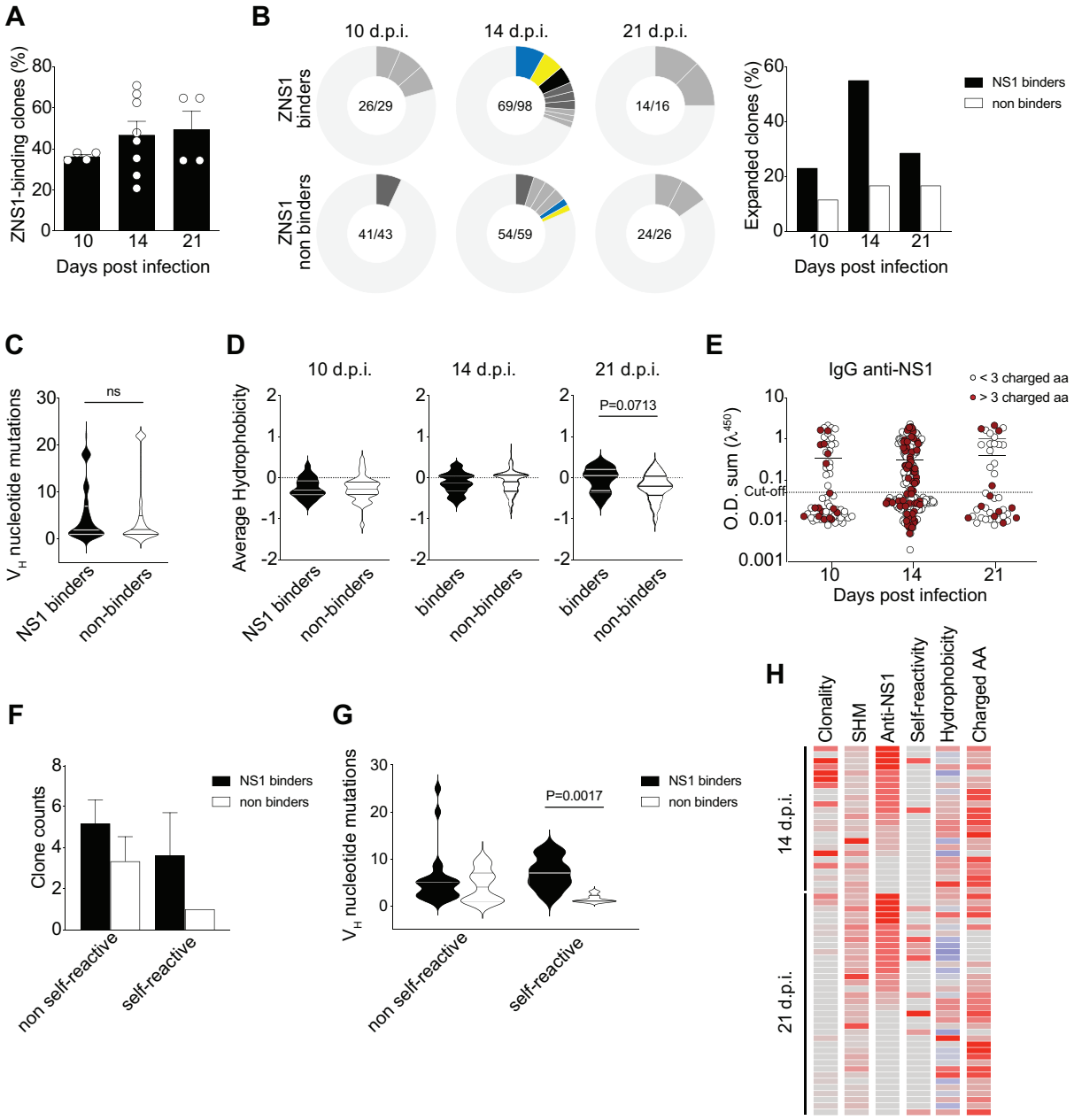

Figure 6. Self-reactivity of GC B after ZIKV NS1 immunization. Single GC B cells were sorted and cultured on a monolayer of gamma-irradiated feeder cells ($1x10^3$ cells/well) expressing CD40L, BAFF and IL-21 (Kuraoka et al., 2016). After 7 days, supernatants were collected for binding assays and cells were harvested for *Igh* sequencing. **(A)** Frequency of IgG^+ single GC B cell culture supernatants that bound to ZIKV NS1. Supernatants were screened for IgG production and IgG^+ wells were tested for binding to ZIKV NS1 protein by ELISA. **(B)** Clonal distribution of GC B cells found to bind to NS1 (upper panel) or that did not bind to NS1 (lower panel). Size of the slice is proportional to the clone frequency. Colored slices represent variants of clones that were found both as binders and non-binders. Right panel represents the frequency of expanded clones among binders and non-binders at

specific time points after immunization. **(C)** Number of somatic mutations found in V_H segments from each GC B cell sequenced grouped based on binding to NS1. **(D)** CDR-H3 average hydrophobicity index variation at different time points grouped based on binding to NS1. **(E)** Distribution of OD in NS1 ELISA with single cell culture supernatants related to the presence of charged amino acids. Red dots indicate the presence of 3 or more charged amino acids in CDR-H3 at different time points. **(F-H)** Single GC B cell culture supernatants were tested for binding to NS1 by ELISA and to self-antigens by immunoblot. **(F)** Clone counts of NS1 binders (black bars) and NS1 non binders (white bars) separated by self-reactivity. **(G)** Number of somatic mutations found in V_H segments from each GC B cell sequenced grouped based on binding to NS1 and self-reactivity assessed by immunoblot. **(H)** Clonality, somatic hypermutation, binding to NS1, self-reactivity, hydrophobicity and charged amino acid usage ploted by time after immunization. Clonality corresponds to the number of variants of each clone found in the dataset. SHM is represented by the number of VH mutations found in each sequence. Anti-NS1 indicates the OD obtained by ELISA. Self-reactivity corresponds to the number of bands found for each supernatant in mouse tissue extracts (brain and/or muscle). Hydrophobicity corresponds to the average hydrophobicity of the CDR-H3 loop, hydrophobic and charged CDR-H3 sequences are shown in blue and red, respectively. Charged AA indicates the number of charged amino acids found in CDR-H3 loop.

Supplementary material

Supplementary Figure 1

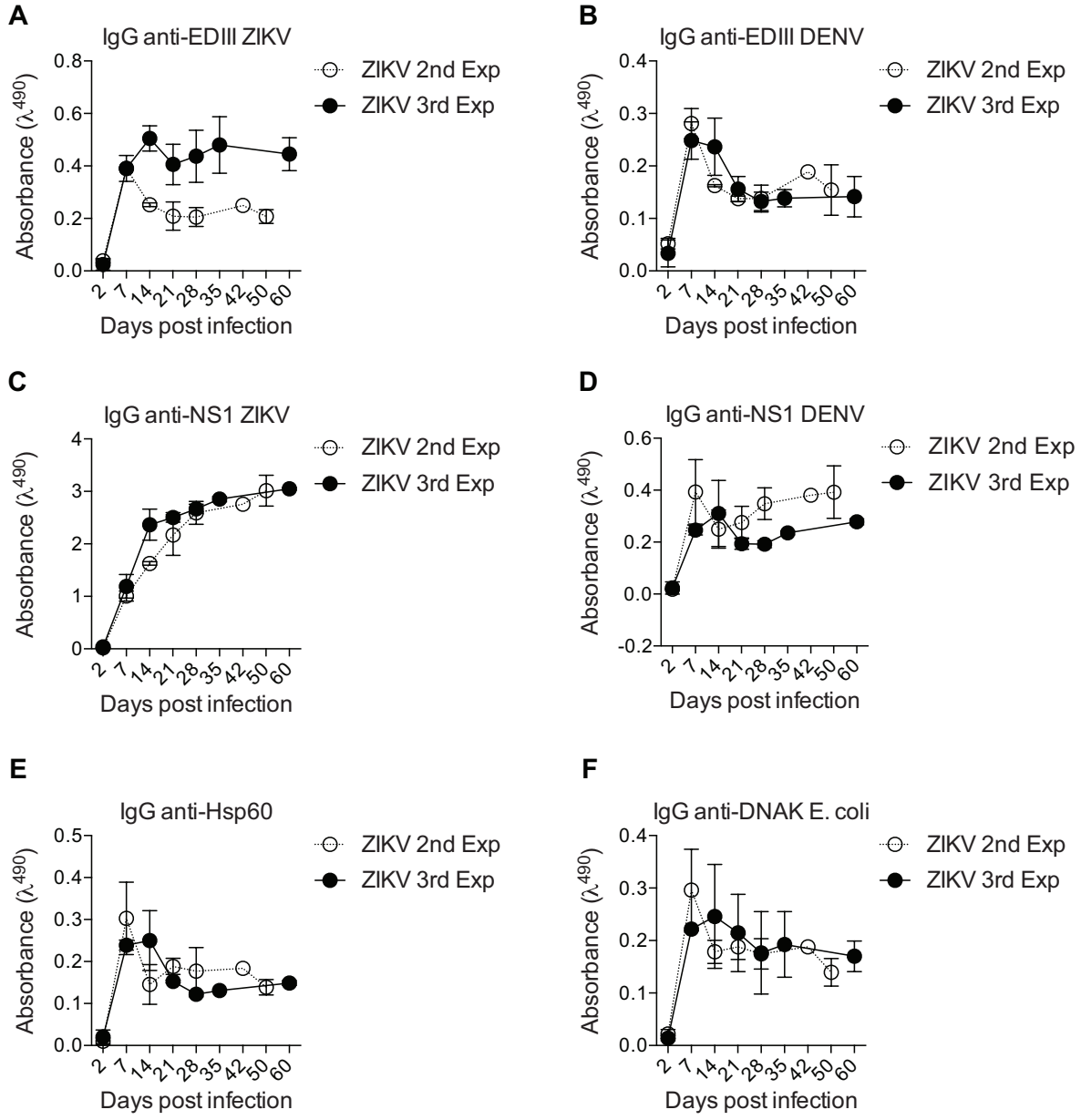

Suppl. figure 1. Cross reactivity with unrelated antigens. Sera from ZIKV infected mice (1:120 dilution) from 2 independent experiments were tested by ELISA for binding to ZIKV and DENV antigens EDIII (**A and B**) and NS1 (**C and D**) as well as unrelated antigens heat-shock protein Hsp60 and bacterial DNAK from E. coli at different time points. 2nd experiment ended at 50 days and 3rd experiment at 60 days.

Supplementary Table 1: CDR-H3 characteristics from germinal center B cell clones tested for self-reactivity.

ID	dpi	CDR-H3	VH	JH	Average hidrophobicity	CDR-H3 loop length	NS1 OD	# of self reactive bands	Immunization antigen
P05B05	14	ARGGGFDGFAY	V1-12	3	0.037	6	1.148	0	ZIKV NS1
P05B06	14	AREDRGFAY	V5-6-3	3	-0.818	4	0.005	0	ZIKV NS1
P05B07	14	ARGGGFDGFAY	V1-12	3	0.037	6	1.491	2	ZIKV NS1
P05B08	14	ARGGGYDGFAY	V1-12	3	-0.192	6	1.096	0	ZIKV NS1
P05C03	14	ARGGGYDGFAY	V1-12	3	-0.192	6	0.850	0	ZIKV NS1
P05C05	14	ARGGGLWGAMDY	V1-87	4	0.307	7	1.256	0	ZIKV NS1
P05C12	14	ARGGGLWGAMDY	V1-87	4	0.307	7	0.080	0	ZIKV NS1
P05D07	14	ARSGGSYDNYDYCSMDY	V1-54	4	-0.254	12	0.664	0	ZIKV NS1
P05E04	14	TRGGGYDYEAWFAY	V5-6-4	3	-0.202	9	0.009	0	ZIKV NS1
P05E07	14	ARGKRDGYYPYAMDY	V2-6-7	4	-0.375	10	0.228	0	ZIKV NS1
P05F01	14	VRGAHYAMDY	V1-7	4	0.078	5	2.276	0	ZIKV NS1
P05F10	14	ARDRATVVADYYTMDY	V2-6-7	4	0.069	11	1.037	0	ZIKV NS1
P05F11	14	AREYYGSTFAY	V1-14	3	-0.280	6	0.164	0	ZIKV NS1
P05G03	14	ARQVRPYAMDY	V3-2	4	-0.095	6	0.008	0	ZIKV NS1
P05G04	14	ARMGLDSSGLYGMDY	V1S132	4	0.222	10	0.226	0	ZIKV NS1
P05G06	14	ARKKDGYAMDY	V2-6-4	4	-0.445	6	0.531	0	ZIKV NS1
P05G08	14	AREYYGSTFAY	V1-14	3	-0.280	6	0.005	0	ZIKV NS1
P05G12	14	VRGQIHYYGPWYFDV	V1-87	1	-0.147	10	0.859	1	ZIKV NS1
P05H03	14	ARGQFHYYGPWYFDV	V1-87	1	-0.207	10	0.841	2	ZIKV NS1
P07A02	14	ARDRYGAMDY	V2-9	4	-0.354	5	2.873	0	ZIKV NS1
P07A05	14	ARDRYGAMDY	V2-9	4	-0.354	5	1.462	0	ZIKV NS1
P07A10	14	ARERYGSSLAY	V1-14	3	-0.457	6	0.369	0	ZIKV NS1
P07B01	14	ARDRYGAMDY	V2-9	4	-0.354	5	0.028	0	ZIKV NS1
P07B12	14	ARDDGYSTYHYAMDY	V1-87	4	-0.309	10	0.039	0	ZIKV NS1
P09A01	21	ARNWDY	V2-2	2	-1.000	1	0.015	0	ZIKV NS1
P09A02	21	ARHGISQAWFAY	V1-54	3	0.050	7	0.253	1	ZIKV NS1
P09A04	21	ARNWAFTY	V1-9	3	-0.123	3	1.852	0	ZIKV NS1
P09A05	21	ARGGGNYVFDY	V1S56	2	0.070	6	0.010	0	ZIKV NS1
P09A07	21	SRGGYDGGAYYFDY	V1-39	2	-0.102	9	0.723	0	ZIKV NS1
P09A08	21	AQQRLPYYFDY	V3-1	2	-0.302	6	2.131	0	ZIKV NS1
P09A09	21	ARDYYGNSFHY	V9-2-1	2	-0.435	6	0.142	0	ZIKV NS1
P09A10	21	ARDYYGNSFSY	V9-2-1	2	-0.435	6	0.204	0	ZIKV NS1
P09A11	21	ARSYDGYLYAMDY	V3-8	4	0.036	8	0.012	0	ZIKV NS1
P09B01	21	ARGTLYTMDY	V1-87	4	0.204	5	0.716	0	ZIKV NS1
P09B02	21	ARGTLYAMDY	V1-87	4	0.372	5	0.756	1	ZIKV NS1
P09B04	21	ARGTLYSMDY	V1-87	4	0.198	5	1.107	2	ZIKV NS1
P09B06	21	VRHGSSWVFDY	V1S40	2	0.063	6	0.518	0	ZIKV NS1
P09E02	21	ARRVYAMDY	V3-2	4	0.200	4	0.009	0	ZIKV NS1
P09E09	21	ARRVYAMDY	V3-2	4	0.200	4	0.011	0	ZIKV NS1
P09E11	21	ARRNWDGGFAY	V5-12-1	3	-0.563	6	0.012	0	ZIKV NS1
P09F01	21	ARGGGNYAVDY	V1-18	4	-0.068	6	0.021	0	ZIKV NS1
P09F02	21	AKEEGGGDYAMDY	V1-7	4	-0.301	8	0.009	1	ZIKV NS1
P09F04	21	SRLTGTYAMDY	V1-55	4	0.298	6	0.732	2	ZIKV NS1
P09F05	21	SRFRYEGDYAMDY	V1-82	4	-0.243	8	0.041	3	ZIKV NS1
P09F08	21	TRRGGNYKFAY	V4-1	3	-0.602	6	1.581	0	ZIKV NS1
P09F10	21	ARGGRYYGSGFVDAMDY	V1-67	4	0.054	12	1.641	1	ZIKV NS1
P09G02	21	ARGGRYYGSGFVDAMDY	V1-67	4	0.054	12	1.365	1	ZIKV NS1
P09G03	21	ARDSNYRFPY	V1-26	3	-0.734	5	0.012	0	ZIKV NS1
P09G04	21	ARGVTGSFDY	V1-54	2	0.298	5	0.019	1	ZIKV NS1
P09G06	21	ARLTGTYAMDY	V1-55	4	0.298	6	0.764	1	ZIKV NS1
P09H01	21	ASDLSYSMDY	V2-9	4	-0.014	5	0.474	0	DENV NS1
P09H06	21	AREGYGNSFDY	V1-14	3	-0.385	6	0.027	0	DENV NS1
P09H11	21	ARRWAYYYGSSGYYFDY	V5-12-1	2	-0.180	12	0.438	0	DENV NS1
P09B08	21	ARLDFIRYGSSYEAMDY	V5-9-2	4	0.080	12	0.013	0	DENV NS1
P09B10	21	ARHYAMDY	V5-12	4	-0.137	3	0.011	0	DENV NS1
P09C01	21	ARLDFIRYGSRYEAMDY	V5-9-2	4	-0.020	12	0.014	0	DENV NS1
P09C02	21	ARTGYDYDSAWFAY	V5-6-5	3	-0.228	9	0.010	0	DENV NS1
P09C06	21	AREEARQLGLFYAMDY	V1-14	4	0.082	11	0.014	0	DENV NS1
P09C07	21	ARSGGYWYFNV	V1S29	1	-0.120	6	1.516	0	DENV NS1
P09D10	21	ARSGGYWYFDV	V1S29	1	-0.120	6	1.319	0	DENV NS1